Inelastic x-ray scattering from phonons under multibeam conditions

Alexey Bosak and Michael Krisch
European Synchrotron Radiation Facility, Boîte Postal 220, F-38043 Grenoble Cedex, France

(Received 22 January 2007; published 16 March 2007)

We report on an experimental observation of a previously neglected multibeam contribution to the inelastic x-ray scattering cross section. Its manifestation is a substantial modification of the apparent phonon selection rules when two (or more) reciprocal lattice points are simultaneously intercepted by the Ewald sphere. The observed multibeam contributions can be treated semi-quantitatively in the frame of Renninger's "simplest approach." A few corollaries, relevant for experimental work on inelastic scattering from phonons, are presented.

DOI: 10.1103/PhysRevB.75.092302 PACS number(s): 61.10.Eq, 63.20.Dj, 78.70.Ck

Since the development of inelastic neutron scattering in the 1950's (Ref. 1) and inelastic x-ray scattering in the 1980's (Ref. 2) these techniques have been extensively used to study the lattice dynamics in a large variety of materials ranging from simple metals to complex biological systems. The experimental observable is the dynamical structure factor $S(\vec{Q},E)$, where $\vec{Q}$ is the momentum transfer (defined as the difference between the incident $\vec{k}_0$ and the scattered x-ray wave vector $\vec{k}_A$), and E is the energy transfer (difference between incident and scattered photon energy). An appropriate orientation of the sample and choice of the scattering geometry allows the mapping of the different phonon branches. Here, E is directly identified with the phonon energy, while the phonon momentum $\vec{q}$ is connected to the total momentum transfer $\vec{Q}$ via a reciprocal lattice vector $\vec{\tau}$.[3] In all previous neutron (except for two cases mentioned below) and x-ray work it was implicitly assumed that for a given experimental setup only one reciprocal lattice vector is involved in the scattering process. On the other hand, it is well known that the Ewald sphere can intercept more than one reciprocal lattice point, giving rise to multibeam diffraction phenomena.[4] This has been exploited in the past, for example, to solve the "phase problem"[5] in crystallography,[6–8] and to provide a full polarization analysis of an x-ray beam.[9]

Here we report an experimental inelastic x-ray scattering (IXS) study of silicon, which shows that the $S(\vec{Q},E)$ is dramatically modified, when going from the conventional two-beam case (involving only the incident and one scattered wave vector) to the three-beam case, for which an additional reciprocal lattice vector is involved in the inelastic scattering process.

The IXS experiments were conducted on beamline ID28 at the European Synchrotron Radiation Facility. The measurements were performed at 17794 eV with an energy resolution of 3.0 meV full width at half maximum (FWHM). The dimensions of the focused x-ray beam were 250×60 μm^2 (horizontal $\times$ vertical, FWHM). Direction and size of the momentum transfer were selected by an appropriate choice of the scattering angle in the horizontal scattering plane and the sample orientation. The momentum resolution was set to 0.2 and 0.7 nm^{-1} in the horizontal and vertical plane, respectively. Further details of the experimental setup can be found elsewhere.[10] The resolution function was experimentally determined from a PMMA sample, kept at 10 K, and at $Q=10$ nm^{-1}. The sample was a single crystal of silicon, with its $(10\bar{1})$ plane normal oriented closely along the vertical direction. An online fluorescent screen, coupled to a CCD camera, allowed the prealignment of the crystal in three-beam diffraction conditions, and the precise sample orientation was achieved by a five-circle goniometer.

Figure 1 shows the scattering geometry. In the standard two-beam case (2BC), the configuration consists of the reciprocal lattice point P (lattice vector $\vec{\tau}$), the wave vector of the incident x-rays $\vec{k}_0$ and the scattered wave vector $\vec{k}_A$, with $\vec{Q}=\vec{\tau}+\vec{q}$. The three-beam case (3BC) is met if, by a rotation around $\vec{Q}$ (angle ψ), the Ewald sphere intersects a second reciprocal lattice point (B lattice vector $\vec{L}=\vec{k}_B-\vec{k}_0$). Thus, the diffracted beam along $\vec{k}_B$ acts as the "incident beam" for the scattering vector $\vec{Q}-\vec{L}$. As "A" does not coincide with a reciprocal lattice point, the intensity transfer from the direct beam into $\vec{k}_A$ is negligible compared to the transfer from the direct beam into $\vec{k}_B$, and the scattered intensity along $\vec{k}_A$ is proportional to

$$S(\vec{Q},\vec{L},E) = S(\vec{Q},E) + \alpha \cdot S(\vec{Q}-\vec{L},E), \qquad (1)$$

where α is a dimensionless coefficient for the reflection of the x-ray beam from the direction $\vec{k}_0$ into $\vec{k}_B$. The second

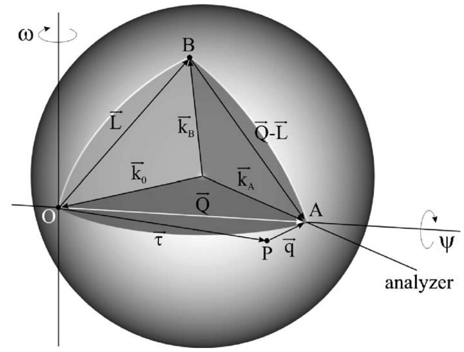

FIG. 1. Scattering geometry in three-beam configuration. The experimental configuration was switched from the three-beam to the two-beam case by a small rotation, $\psi=0.01°$, around the momentum transfer vector $\vec{Q}$. Points O, B, and P are reciprocal lattice points.

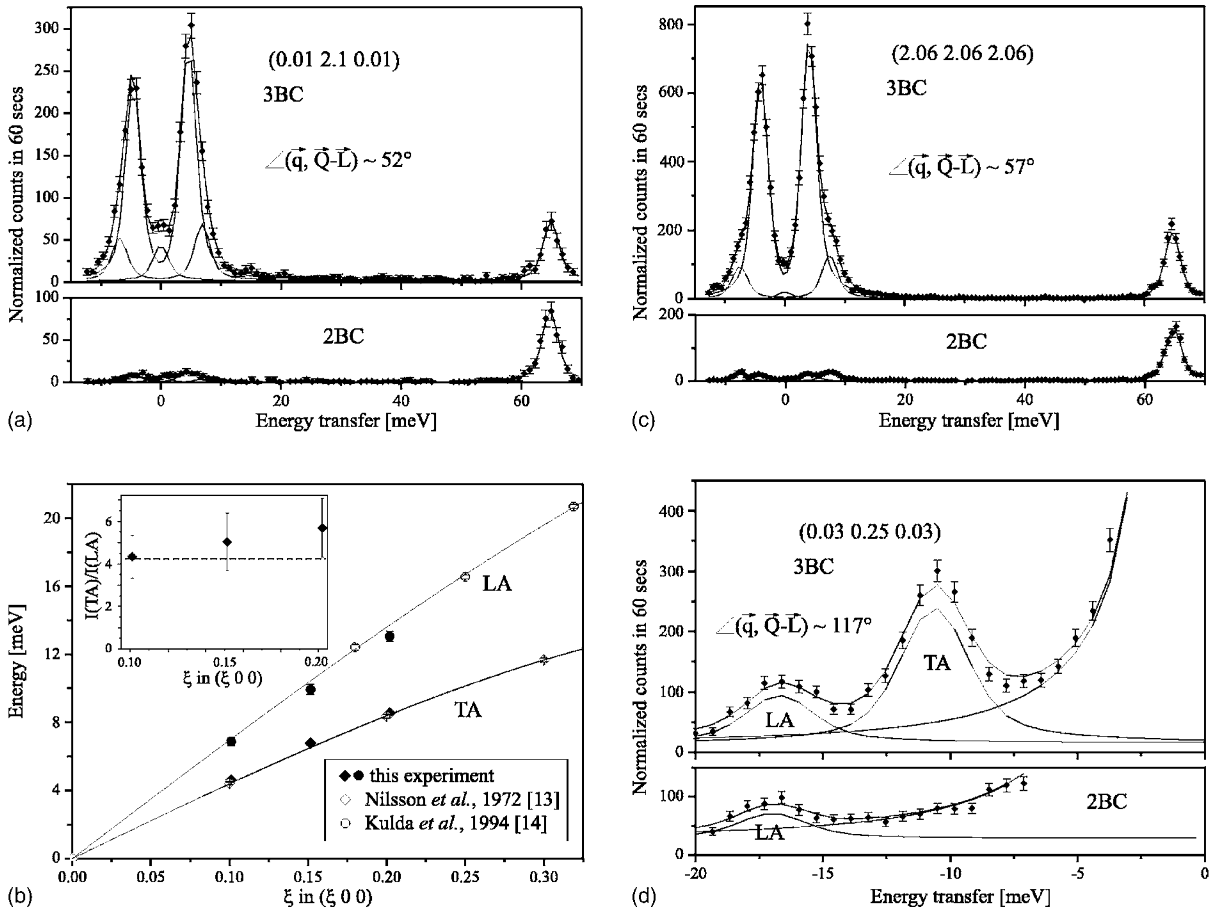

FIG. 2. IXS study performed on a silicon single crystal. (a) IXS spectra, recorded at (0.01 2.1 0.01) in three-beam (top panel) and standard two-beam conditions ($\Delta\psi = 0.01°$) (bottom panel). (b) Acoustic phonon dispersion in the proximity of the (0 2 0) reciprocal lattice point (full symbols) compared to INS data (open symbols). In the inset the experimental ratio $I(\mathrm{TA})/I(\mathrm{LA})$ is compared to the calculated one (dashed line). (c) IXS spectra, recorded at (2.06 2.06 2.06) in three-beam (top panel) and standard two-beam conditions ($\Delta\psi = 0.01°$) (bottom panel). (d) IXS spectra at (0.03 0.25 0.03) in three-beam (top panel) and standard two-beam conditions ($\Delta\psi = 0.01°$) (bottom panel). The experimental IXS spectra are shown together with the best fit results, using a set of experimental resolution functions.

term resembles the *Umweganregung* term in Renninger's "simplest approach,"[11] but includes the energy dependence of the resulting signal. The intensity in the outgoing beam is the sum over two-beam and three-beam paths. In some sense the present situation can be considered as a multiple scattering process.

IXS spectra were investigated in three configurations as described below.

(i) Absolutely forbidden reflection. The (200) reflection of silicon is absolutely forbidden and can be observed only under multibeam diffraction conditions.[12] The chosen three-beam configuration was

$$\vec{Q}/\vec{L}/\vec{Q}-\vec{L} \approx (0\ 2+\xi\ 0)/(11\bar{1})/(\bar{1}\ 1+\xi\ 1).$$

As can be seen in Fig. 2(a), the acoustic phonons possess significant intensity only if the three-beam condition is met, while the intensity of the longitudinal optic phonons remains unchanged. When the transferred energy is fixed to the acoustic phonon energy, the observed FWHM of ψ scan was about 0.004°. The acoustic phonon dispersion was determined in the proximity of the (0 2 0) reflection; the phonon energies are very close to those determined previously by inelastic neutron scattering,[13,14] as shown in Fig. 2(b). Not only the scattering from the acoustic phonons near the forbidden reflection is unnatural, but also the symmetry-linked selection rules are violated, as for $(0\ k+\xi\ 0)$ in 2BC conditions only longitudinal phonons are observable. The 3BC IXS spectra are, however, dominated by transverse acoustic (TA) phonons, as the comparison with neutron results reveal. The reason is the noncollinearity of the reduced momentum transfer and the 3BC momentum transfer $\vec{Q}-\vec{L}$. As the IXS cross section is, amongst others, proportional to the scalar product of the phonon eigenvector and the momentum transfer [see Eq. (3) below], both longitudinal and transverse phonon modes acquire significant intensity. The observed $I(\mathrm{TA})/I(\mathrm{LA})$ ratio is very close to the one calculated in the low-energy limit from the *Umweganregung*-linked geometric factor $G(\vec{Q}-\vec{L},TA)/G(\vec{Q}-\vec{L},LA) \approx 2$ plus thermal factors $F(E,T,\vec{Q},TA)/F(E,T,\vec{Q},LA) \approx C_{11}/C_{44} \approx 2.08$ [see inset of Fig. 2(b)]. The deviation increases for larger momentum transfer as the elastic approximation loses its validity, and knowledge of the real lattice dynamics is needed for the quantitative treatment. Here, we utilized the formalism for $S(\vec{Q},E)$ within the limit of one-phonon scattering[15]

$$S(\vec{Q},E) = \sum_j G(\vec{Q},j)F(E,T,\vec{Q},j), \tag{2}$$

$$G(\vec{Q},j) = \left| \sum_n f_n(\vec{Q}) e^{-W_n(\vec{Q})+i\vec{Q}\cdot\vec{r}_n}[\vec{Q}\cdot\hat{\sigma}_n(\vec{q},j)]M_n^{-1/2}\right|^2 \tag{3}$$

and the thermal factor

$$F(E,T,\vec{Q},j) = \frac{\left[\exp\left(\frac{E_{\vec{q},j}}{kT}\right)-1\right]^{-1}+\frac{1}{2}\pm\frac{1}{2}}{E_{\vec{q},j}}\delta(E\mp E_{\vec{q},j}), \tag{4}$$

where $\vec{Q}=\vec{q}+\vec{\tau}$ denotes the momentum transfer, the sum extends over atoms in the unit cell, $f_n(\vec{Q})=f_n(|\vec{Q}|)\equiv f_n(Q)$ is the atomic form factor of atom n at position $\vec{r}_n$, $\hat{\sigma}_n(\vec{q}+\vec{\tau},j)=\hat{\sigma}_n(\vec{q},j)$ is its eigenvector component in mode j, M_n its mass, and W_n the corresponding Debye-Waller factor.

(ii) Nearly forbidden reflection. The (222) reflection of silicon is formally forbidden, but still acquires some intensity due to charge asymmetries introduced by the covalent bonds (dominating contribution at room temperature).[16] Indeed, in 2BC conditions the intensity of the (222) reflection is two orders of magnitude weaker than adjacent allowed reflections, and in its proximity no significant contribution of acoustic phonons to the inelastic scattering is expected. The chosen three-beam configuration was

$$\vec{Q}/\vec{L}/\vec{Q}-\vec{L} \approx (2+\xi\ 2+\xi\ 2+\xi)/(\bar{1}13)/(3+\xi\ 1+\xi\ \bar{1}+\xi).$$

As in the previous case, the intensity scattered from the acoustic phonons disappears very rapidly with a small rotation in ψ [Fig. 2(c)], while the optical phonon intensity remains unchanged, since it is determined mainly by the direct channel [first term of Eq. (1)].

(iii) Proximity of the direct beam. As in the first Brillouin zone momentum transfer and reduced momentum transfer coincide ($\vec{Q}=\vec{q}$), only scattering from longitudinal phonons is allowed along high-symmetry directions, but this selection rule again can be violated *via* multibeam processes. The chosen three-beam configuration was

$$\vec{Q}/\vec{L}/\vec{Q}-\vec{L}=\vec{q}/\vec{L}/\vec{q}-\vec{L} \approx (0\ \xi\ 0)/(11\bar{1})/(\bar{1}\ \bar{1}+\xi\ 1).$$

For selected ψ values, the TA phonon intensity can exceed that of the LA phonon, and the intensity of the LA phonon is in turn modified as contributions from both channels contribute [Fig. 2(d)]. As $|\vec{q}-\vec{L}|\gg|\vec{q}|$ and $I\propto|\vec{Q}|^2$, the 3BC contribution can become dominating.

To our knowledge, similar features were reported only for INS experiments performed on lead[17] and bismuth.[18] As in our case, for longitudinal scattering geometry additional "anomalous neutron groups" were observed which apparently correspond to transverse phonons of the same $\vec{q}$. These were ascribed to a double scattering process.[17]

Our findings have several consequences. Attention has to be paid, when a full determination of the lattice dynamics (knowledge of phonon eigenfrequencies and eigenvectors) shall be performed. To this purpose accurate measurements of the scattered intensity of various phonon modes are necessary.[19] The accidental contribution of multibeam processes can seriously alter the analysis, and need therefore to be avoided, as is common practice in crystallography. The lower is the crystal symmetry, the larger is the lattice parameter, and the more the problem will become serious. Furthermore, the double scattering events should become more probable with increasing mosaic spread, and, consequently, angular acceptance of the reflection.

Despite the fact that a simple kinematic approach describes the observed phenomena strikingly well, for perfect crystals a treatment within the frame of dynamical theory is highly desirable.[20] The change in $|\vec{k}|$ can be mostly neglected, in contrast to neutron inelastic scattering. For example, the Darwin width for the silicon (111) reflection at 17.8 keV is ~3 arcsec, while even for the largest phonon energy transfer in silicon the $|\vec{k}|$ variation corresponds to an angular spread of less than 0.1 arcsec for the same angular range. Only the full dynamical treatment can give the appropriate values for the absolute intensities of phonons in the 3BC and correct angular widths of elastic and inelastic features. One might speculate that this gives access to further information such as the phase of the phonon eigenvectors. Finally, for high-pressure IXS experiments on polycrystalline, glassy or liquid samples in diamond anvil cells, performed within the first Brillouin zone, the contribution of the diamond TA peak can interfere with the inelastic feature of interest.[21] In many cases its intensity is anomalously high, and cannot be explained by normal scattering mechanisms. The most probable mechanism is the three-beam case phenomenon, and a ψ correction seems to be an adequate solution; the magnitude of necessary correction should remain small, well below 0.1°.

A. Bosak is grateful to D. Chernyshov (The Suiss-Norvegian Beamlines at ESRF) for the numerous fruitful discussions and to B. Dorner and R. Currat (Institut Laue-Langevin, Grenoble, France) for many useful suggestions.

[1] B. N. Brockhouse, Can. J. Phys. **33**, 889 (1955).
[2] B. Dorner, E. Burkel, Th. Illini, and J. Peisl, Z. Phys. B: Condens. Matter **69**, 179 (1987).
[3] G. L. Squires, *Introduction to the Theory of Thermal Neutron Scattering* (Cambridge University Press, Cambridge, 1978).
[4] P. P. Ewald, Rev. Mod. Phys. **37**, 46 (1965).
[5] *Modern Crystallography I, Springer Series in Solid-State Sciences* (Springer Verlag, Berlin, 1981), Vol. 15.
[6] R. Colella, Acta Crystallogr., Sect. A: Cryst. Phys., Diffr., Theor. Gen. Crystallogr. **30**, 413 (1974).

[7] B. Post, Phys. Rev. Lett. **39**, 760 (1977).

[8] E. Weckert and K. Hümmer, Acta Crystallogr., Sect. A: Found. Crystallogr. **53**, 108 (1997).

[9] Q. Shen and K. D. Finkelstein, Phys. Rev. B **45**, 5075(R) (1992).

[10] M. Krisch, J. Raman Spectrosc. **34**, 628 (2003).

[11] E. Rossmanith, J. Appl. Crystallogr. **33**, 921 (2000).

[12] J. Z. Tischler, J. D. Budai, G. E. Ice, and A. Habenschuss, Acta Crystallogr., Sect. A: Found. Crystallogr. **44**, 22 (1988).

[13] G. Nilsson and G. Nelin, Phys. Rev. B **6**, 3777 (1972).

[14] J. Kulda, D. Strauch, P. Pavone, and Y. Ishii, Phys. Rev. B **50**, 13347 (1994).

[15] E. Burkel, Rep. Prog. Phys. **63**, 171 (2000).

[16] J. B. Roberto and B. W. Batterman, Phys. Rev. B **2**, 3220 (1970).

[17] B. N. Brockhouse, T. Arase, G. Caglioti, M. Sakatomo, R. N. Sinclair, A. D. B. Woods, *Inelastic Scattering of Neutrons in Solids and Liquids* (International Atomic Energy Agency, Vienna, 1961), p. 531; B. N. Brockhouse, T. Arase, G. Caglioti, K. R. Rao, and A. D. B. Woods, Phys. Rev. **128**, 1099 (1962).

[18] J. L. Yarnell, J. L. Warren, R. G. Wenzel, and S. H. Koenig, IBM J. Res. Dev. **8**, 234 (1964).

[19] D. Strauch and B. Dorner, J. Phys. C **19**, 2853 (1986).

[20] B. W. Batterman and H. Cole, Rev. Mod. Phys. **36**, 681 (1964).

[21] D. Antonangeli, M. Krisch, G. Fiquet, J. Badro, D. L. Farber, A. Bossak, and S. Merkel, Phys. Rev. B **72**, 134303 (2005).